Progress of Theoretical Physics, Vol. 128, No. 5, November 2012

Gravitational Waves from a Particle in Circular Orbits around a Schwarzschild Black Hole to the 22nd Post-Newtonian Order

Ryuichi FUJITA[1,2]

[1]*Departament de Física, Universitat de les Illes Balears, Cra. Valldemossa Km. 7.5, Palma de Mallorca, E-07122, Spain*
[2]*Raman Research Institute, Bangalore 560 080, India*

(Received August 25, 2012)

We extend our previous results of the 14th post-Newtonian (PN) order expansion of gravitational waves for a test particle in circular orbits around a Schwarzschild black hole to the 22PN order, i.e. v^{44} beyond the leading Newtonian approximation where v is the orbital velocity of a test particle. Comparing our 22PN formula for the energy flux with high precision numerical results, we find that the relative error of the 22PN flux at the innermost stable circular orbit is about 10^{-5}. We also estimate the phase difference between the 22PN waveforms and numerical waveforms after a two-year inspiral. We find that the dephase is about 10^{-9} for $\mu/M = 10^{-4}$ and 10^{-2} for $\mu/M = 10^{-5}$ where μ is the mass of the compact object and M the mass of the central supermassive black hole. Finally, we construct a hybrid formula of the energy flux by supplementing the 4PN formula of the energy flux for circular and equatorial orbits around a Kerr black hole with all the present 22PN terms for the case of a Schwarzschild black hole. Comparing the hybrid formula with the the full numerical results, we examine the performance of the hybrid formula for the case of Kerr black hole.

Subject Index: 420, 452

§1. Introduction

Gravitational waves (GWs) are expected to be detected in this decade by upcoming ground based detectors such as Advanced LIGO,[1)] VIRGO[2)] and KAGRA.[3)] One of the most promising sources of the GWs for the ground based detectors is the coalescing stellar-mass compact object binary system. For the detection of the GWs and the subsequent parameter estimation of the source, one will correlate the noisy signal of the detector with the template bank of theoretical waveforms. Thus, it is important to predict the waveforms very accurately and efficiently not only for developing the data analysis strategy but also for extracting the physical information of the source.

A conventional method to predict inspiral waveforms from coalescing binaries is the post-Newtonian (PN) expansion of the Einstein equations,[4)] in which the relative velocity of the binary v is assumed to be smaller than the speed of light. Currently, the amplitude (orbital phase) of gravitational waves is derived up to 3PN (3.5PN), i.e. v^6 (v^7) beyond the leading order,[5)–11)] for the non-spinning compact binaries in quasi-circular orbits. (Note that the 3.5PN amplitude for $\ell = m = 2$ mode is derived in Ref. 12).) Although the PN expansion accurately describes the early phase of the inspiral, the approximation breaks down in the late phase of the inspiral. For the late inspiral and the subsequent merger and ringdown phases one needs to calculate the

waveforms using a full numerical solution of the Einstein equations.[13),14)] Since the computational cost to perform full numerical simulations which include the whole process of the coalescence is too expensive, one should make theoretical templates by matching the PN waveforms in the early inspiral phase with the numerical waveforms in the late inspiral and the subsequent merger and ringdown phases.[15),16)] Thus, from the point of view of the computational cost it is important to obtain higher PN order expressions of the GWs and to investigate whether the high PN order expressions extend the region where the PN expansions of GWs are sufficiently reliable.

For this purpose, we derive the high PN order expressions of the GWs focusing on a binary system which consists of a compact object of mass μ in circular orbits around a Schwarzschild black hole of mass M by assuming $\mu \ll M$. Such extreme mass ratio inspirals (EMRIs) are one of the main candidates of gravitational waves for space-based detector such as eLISA.[17)] Another approach to model EMRIs is the black hole perturbation formalism, which uses the mass ratio as an expansion parameter. Although the black hole perturbation theory is limited to the case $\mu \ll M$, it is rather easier to compute the high PN order expansions of the GWs than using the standard PN approximation. Moreover, one can use the numerical results of the black hole perturbation theory to investigate the relative accuracy of the PN expansions since in the black hole perturbation theory there are no assumptions on the orbital velocity of the compact object.

Using the first order black hole perturbation theory, the gravitational waveforms and energy flux to infinity for a test particle in circular orbits around a Schwarzschild black hole were computed up to 1.5PN in Ref. 18). (See Refs. 19)–21) for recent reviews for orbital evolution due to the small body's interaction with its own gravitational field, i.e. gravitational self-force.) The calculation of the energy flux is extended up to 2.5PN by numerical fitting in Ref. 22). Then, in Ref. 23) the 4PN expressions of the energy flux were derived by fitting with a very accurate numerical calculation of the energy flux. It was also found that $\log v$ terms appear at 3PN and 4PN in Ref. 23). These $\log v$ terms were confirmed in Ref. 24), which computed analytically the 4PN expressions of the energy flux. These calculations were extended to 5.5PN for the energy flux in Ref. 25) and for the waveforms in Ref. 26). Recently the 14PN gravitational waveforms for a test particle in circular orbits around a Schwarzschild black hole have been derived.[27)] By comparing the 14PN energy flux with numerical results, it is shown that the relative error of the post-Newtonian energy flux becomes smaller when the PN order is higher. It is also shown that the 14PN waveforms using factorized resummation suggested in Ref. 28) will provide the data analysis performances of EMRIs comparable to the ones resulting from high precision numerical waveforms. In this paper we extend the 14PN results in Ref. 27) to the 22PN, which is the highest order we can derive with reasonable time using our current code.[*)] We find that if one does not use any re-

[*)] We note that the number of terms necessary to derive the PN expressions grows exponentially when the PN order becomes higher. Our current code uses 70, 3.3×10^2, 1.9×10^3, 1.1×10^4 and 3.3×10^4 MBytes memory, taking seconds to a few days, to compute multipolar waveforms for $\ell = m = 2$ mode at 6PN, 10PN, 14PN, 18PN and 22PN respectively. Thus, it is difficult to obtain 23PN or higher order expressions with reasonable time by using our current code.

summation technique the 22PN gravitational waveforms will be necessary to achieve the data analysis accuracies comparable to the ones using high precision numerical waveforms.

This paper is organized as follows. In §2, we start with a brief summary of the first order black hole perturbation formalism. Section 3 describes a brief summary of an analytic formalism to compute homogeneous solutions of the Teukolsky equation. Section 4 is devoted to the comparison of our 22PN expressions with high precision numerical results: The total energy flux to infinity is compared in §4.1, the phase of gravitational waveforms during two-year inspiral §4.2 and the total energy flux to infinity for the case of a Kerr black hole §4.3. We conclude with a brief summary in §5. Since the 22PN expressions are too large to be shown in the paper, we only show the 7PN expression of the total energy flux to infinity in Appendix A. In Appendix B we show the 22PN expression of the total energy flux to infinity, which can be used for numerical computation in double precision. The 22PN expressions for the modal energy flux to infinity and factorized waveforms[28] will be publicly available online.[29] Throughout this paper, we work in the units of $c = G = 1$.

§2. Teukolsky formalism

We consider the gravitational waves emitted by a test particle moving on circular orbits around a Schwarzschild black hole using the Teukolsky formalism.[30] In this section, we recapitulate necessary equations following the notation in Ref. 31).

In the Teukolsky formalism, the gravitational perturbation of a Schwarzschild black hole is represented by the Weyl scalar Ψ_4, which represents the gravitational waves going out to infinity as

$$\Psi_4 \to \frac{1}{2}(\ddot{h}_+ - i\,\ddot{h}_\times) \ \text{ for } \ r \to \infty, \tag{2·1}$$

where the dot $\dot{}$ represents a time derivative, d/dt.

The Weyl scalar can be separated into radial and angular parts if we decompose Ψ_4 in Fourier harmonic components as

$$\Psi_4 = \frac{1}{r^4}\sum_{\ell,m}\int_{-\infty}^{\infty} d\omega e^{-i\omega t} R_{\ell m\omega}(r)\ {}_{-2}Y_{\ell m}(\theta,\varphi), \tag{2·2}$$

where $\ell \geq 2$, $-\ell \leq m \leq \ell$ and ${}_sY_{\ell m}(\theta,\varphi)$ is the spin-weighted spherical harmonics.[9] The radial function $R_{\ell m\omega}(r)$ satisfies the inhomogeneous Teukolsky equation,

$$\left[\Delta^2 \frac{d}{dr}\left(\frac{1}{\Delta}\frac{d}{dr}\right) + U(r)\right] R_{\ell m\omega}(r) = T_{\ell m\omega}(r), \tag{2·3}$$

with $\Delta = r(r-2M)$ and

$$U(r) = \frac{r^2}{\Delta}\left[\omega^2 r^2 - 4i\omega(r-3M)\right] - (\ell-1)(\ell+2), \tag{2·4}$$

where $T_{\ell m\omega}$ is the source term which is constructed from the energy momentum tensor of the small particle.

We use the Green function method to solve the inhomogeneous Teukolsky equation Eq. (2·3). The outgoing-wave solution of the Teukolsky equation Eq. (2·3) at infinity is given by

$$R_{\ell m\omega}(r\to\infty) = \frac{r^3 e^{i\omega r^*}}{2i\omega B^{\rm inc}_{\ell m\omega}} \int_{2M}^{\infty} dr \frac{R^{\rm in}_{\ell m\omega} T_{\ell m\omega}(r)}{\Delta^2}, \\ \equiv r^3 e^{i\omega r^*} \tilde{Z}_{\ell m\omega}, \tag{2·5}$$

where $r^* = r + 2M\ln(r/2M-1)$ and $R^{in}_{\ell m\omega}$ is the homogeneous solution of Eq. (2·3) which satisfies the ingoing-wave boundary condition at the horizon as

$$R^{\rm in}_{\ell m\omega} = \begin{cases} B^{\rm trans}_{\ell m\omega}\Delta^2 e^{-i\omega r^*} & \text{for} \quad r^*\to-\infty, \\ r^3 B^{\rm ref}_{\ell m\omega} e^{i\omega r^*} + r^{-1} B^{\rm inc}_{\ell m\omega} e^{-i\omega r^*} & \text{for} \quad r^*\to+\infty. \end{cases} \tag{2·6}$$

When the test particle moves on a circular orbit around a Schwarzschild black hole, the angular frequency Ω, the specific energy $\tilde{E}$ and the angular momentum $\tilde{L}$ of the particle are given by

$$\Omega = \sqrt{\frac{M}{r_0^3}}, \quad \tilde{E} = \frac{r_0 - 2M}{\sqrt{r_0(r_0-3M)}}, \quad \tilde{L} = \frac{\sqrt{Mr_0}}{\sqrt{1-3M/r_0}}, \tag{2·7}$$

where r_0 is the orbital radius. The frequency spectrum of $T_{\ell m\omega}$ has peaks at the harmonics of the orbital frequency $\omega = m\Omega$. Then one finds that $\tilde{Z}_{\ell m\omega}$ in Eq. (2·5) takes the form

$$\tilde{Z}_{\ell m\omega} = Z_{\ell m\omega}\delta(\omega - m\Omega), \tag{2·8}$$

where

$$Z_{\ell m\omega} = \frac{\mu\pi}{i\omega(r_0/M)^2 B^{\rm inc}_{\ell m\omega}} \Bigg[\Bigg\{ -{}_0b_{\ell m} - 2\,i\,{}_{-1}b_{\ell m}\left(1 + \frac{i\,\omega\,r_0^2}{2\,(r_0-2M)}\right) \\ + i\,{}_{-2}b_{\ell m}\frac{\omega\,r_0}{(1-2M/r_0)^2}\left(1 - \frac{M}{r_0} + \frac{1}{2}i\,\omega\,r_0\right)\Bigg\} R^{\rm in}_{\ell m\omega} \\ + \left\{ i\,{}_{-1}b_{\ell m} - {}_{-2}\,b_{\ell m}\left(1 + \frac{i\,\omega\,r_0^2}{r_0-2M}\right)\right\} r_0\, R^{\rm in}_{\ell m\omega}{}'(r_0) \\ + \frac{1}{2}{}_{-2}b_{\ell m}\, r_0^2\, R^{\rm in}_{\ell m\omega}{}''(r_0)\Bigg], \tag{2·9}$$

and the prime $'$ denotes differentiation with respect to r and ${}_sb_{\ell m}$ are defined by

$${}_0b_{\ell m} = \frac{1}{2}\left[(\ell-1)\ell(\ell+1)(\ell+2)\right]^{1/2}{}_0Y_{\ell m}\left(\frac{\pi}{2}, 0\right)\frac{\tilde{E}r_0}{r_0-2M}, \tag{2·10a}$$

$${}_{-1}b_{\ell m} = \left[(\ell-1)(\ell+2)\right]^{1/2}{}_{-1}Y_{\ell m}\left(\frac{\pi}{2}, 0\right)\frac{\tilde{L}}{r_0}, \tag{2·10b}$$

$${}_{-2}b_{\ell m} = {}_{-2}Y_{\ell m}\left(\frac{\pi}{2}, 0\right)\tilde{L}\Omega. \tag{2·10c}$$

Using the amplitudes $Z_{\ell m\omega}$, the gravitational wave luminosity is given by

$$\frac{dE}{dt} = \sum_{\ell=2}^{\infty} \sum_{m=-\ell}^{\ell} \frac{|Z_{\ell m\omega}|^2}{4\pi\omega^2}. \tag{2·11}$$

Choosing (θ, φ) as the angles defining the location of the observer relative to the source, the gravitational waveforms can be expressed as

$$h_+ - i\, h_\times = -\frac{2}{r} \sum_{\ell,m} \frac{Z_{\ell m\omega}}{\omega^2}\, {}_{-2}Y_{\ell m}(\theta, \varphi)\, e^{i\omega(r^*-t)}, \tag{2·12}$$

where $\omega = m\Omega$ is the frequency of the gravitational waves.

We derive the post-Newtonian expansions of the gravitational wave luminosity Eq. (2·11) and gravitational waveforms Eq. (2·12) by computing the amplitude $Z_{\ell m\omega}$. For the computation of $Z_{\ell m\omega}$, one needs to obtain the series expansion of the ingoing-wave Teukolsky function $R^{\rm in}_{\ell m\omega}$ in terms of $\epsilon \equiv 2M\omega = 2Mm\Omega = O(v^3)$ and $z \equiv \omega r = O(v)$ and the asymptotic amplitudes $B^{\rm inc}_{\ell m\omega}$ in terms of ϵ, where $v = (M/r_0)^{1/2}$. We use a formalism developed by Mano, Suzuki and Takasugi[32),33)] to compute $R^{\rm in}_{\ell m\omega}$ and $B^{\rm inc}_{\ell m\omega}$. In the next section, we give a brief review of the formalism for the reader's convenience.

§3. Analytic solutions of the homogeneous Teukolsky equation

We adopt the formalism developed by Mano, Suzuki and Takasugi (MST) [32),33)] to obtain the high post-Newtonian order expansion of gravitational waves. In the MST formalism, the homogeneous solutions of the Teukolsky equation are expressed using hypergeometric functions around the horizon and Coulomb wave functions around infinity. Since the matching of the two kinds of solutions can be done analytically in the overlapping region of convergence, one can obtain analytic expressions of the homogeneous solutions without numerical integration. Moreover, the series expansions are naturally related to the low frequency expansion (see §3.2). Thus, the formalism is very powerful to compute the high post-Newtonian order expansion of gravitational waves. Using the MST formalism, the energy absorption of gravitational waves into the horizon induced by a particle in circular orbits around the equatorial plane of a Kerr black hole was calculated up to 6.5PN order beyond the quadrupole formula.[34)] The energy flux of gravitational waves to infinity by a particle in slightly eccentric and inclined orbits around a Kerr black hole was also computed up to 2.5PN order in Refs. 35) and 36). In Refs. 26) and 37), the author of this paper was part of collaborations that applied the formalism to obtain gravitational waveforms for a test particle in circular orbits around a Schwarzschild black hole up to 5.5PN and a Kerr black hole up to 4PN. Extending the formalism to very high post-Newtonian order, we derived the 14PN expressions of gravitational waves for a test particle in circular orbits around a Schwarzschild black hole in Ref. 27). Although the MST formalism can be applied to the case of a Kerr black hole, we set $q = 0$, where q is the non-dimensional spin parameter of the Kerr black hole, since

we are dealing with the case of a Schwarzschild black hole in this paper. We refer the interested reader to a review Ref. 31) for details of the formalism.

3.1. *Ingoing-wave solution*

A homogeneous solution of the Teukolsky equation in a series of Coulomb wave functions $R^{\nu}_{\rm C}$ is defined as

$$R^{\nu}_{\rm C} = z\left(1-\frac{\epsilon}{z}\right)^{2-i\epsilon}\sum_{n=-\infty}^{\infty}(-i)^n\frac{(\nu-1-i\epsilon)_n}{(\nu+3+i\epsilon)_n}a^{\nu}_n F_{n+\nu}(2\,i-\epsilon,z), \tag{3·1}$$

where $z=\omega r$, $(a)_n=\Gamma(a+n)/\Gamma(a)$, and $F_N(\eta,z)$ is a Coulomb wave function defined by

$$F_N(\eta,z)=e^{-iz}2^N z^{N+1}\frac{\Gamma(N+1-i\eta)}{\Gamma(2N+2)}\Phi(N+1-i\eta,2N+2;2iz), \tag{3·2}$$

where $\Phi(\alpha,\beta;z)$ is a confluent hypergeometric function.[38] Observe that the so-called renormalized angular momentum ν is introduced in the homogeneous solution in a series of Coulomb wave functions Eq. (3·1). This parameter ν is a generalization of ℓ and $\nu\to\ell$ as $\epsilon\to 0$. The parameter is determined by the conditions that the series converges and actually represents a homogeneous solution of the Teukolsky equation.

Substituting the solution in a series of Coulomb wave functions Eq. (3·1) into the Teukolsky equation Eq. (2·3) with $T_{\ell m\omega}=0$, we obtain a three-term recurrence relation for the expansion coefficients a^{ν}_n

$$\alpha^{\nu}_n a^{\nu}_{n+1}+\beta^{\nu}_n a^{\nu}_n+\gamma^{\nu}_n a^{\nu}_{n-1}=0, \tag{3·3}$$

where

$$\alpha^{\nu}_n=\frac{i\epsilon(n+\nu-1+i\epsilon)(n+\nu-1-i\epsilon)(n+\nu+1+i\epsilon)}{(n+\nu+1)(2n+2\nu+3)}, \tag{3·4a}$$

$$\beta^{\nu}_n=-\ell(\ell+1)+(n+\nu)(n+\nu+1)+2\epsilon^2+\frac{\epsilon^2(4+\epsilon^2)}{(n+\nu)(n+\nu+1)}, \tag{3·4b}$$

$$\gamma^{\nu}_n=-\frac{i\epsilon(n+\nu+2+i\epsilon)(n+\nu+2-i\epsilon)(n+\nu-i\epsilon)}{(n+\nu)(2n+2\nu-1)}. \tag{3·4c}$$

The series Eq. (3·1) converges if the renormalized angular momentum ν satisfies the following equation,[31),32)]

$$R_n L_{n-1}=1, \tag{3·5}$$

where R_n and L_n are defined by continued fractions, which are derived by the three-term recurrence relation Eq. (3·3), as

$$R_n\equiv\frac{a^{\nu}_n}{a^{\nu}_{n-1}}=-\frac{\gamma^{\nu}_n}{\beta^{\nu}_n+\alpha^{\nu}_n R_{n+1}}=-\frac{\gamma^{\nu}_n}{\beta^{\nu}_n-}\,\frac{\alpha^{\nu}_n\gamma^{\nu}_{n+1}}{\beta^{\nu}_{n+1}-}\,\frac{\alpha^{\nu}_{n+1}\gamma^{\nu}_{n+2}}{\beta^{\nu}_{n+2}-}\cdots, \tag{3·6}$$

$$L_n \equiv \frac{a_n^\nu}{a_{n+1}^\nu} = -\frac{\alpha_n^\nu}{\beta_n^\nu + \gamma_n^\nu L_{n-1}} = -\frac{\alpha_n^\nu}{\beta_n^\nu -}\,\frac{\alpha_{n-1}^\nu \gamma_n^\nu}{\beta_{n-1}^\nu -}\,\frac{\alpha_{n-2}^\nu \gamma_{n-1}^\nu}{\beta_{n-2}^\nu -}\cdots . \tag{3·7}$$

From the continued fractions, R_n and L_n, one can obtain two kinds of the expansion coefficients, a_n^ν. In general, these two kinds of the expansion coefficients do not coincide. Equation (3·5) is a condition such that the two types of the expansion coefficients coincide and the series converges.[31),32)] If we choose ν using Eq. (3·5), the series of Coulomb wave function Eq. (3·1) converges for $r > r_+$. From Eq. (3·4), we find $\alpha_{-n}^{-\nu-1} = \gamma_n^\nu$ and $\beta_{-n}^{-\nu-1} = \beta_n^\nu$ so that $a_{-n}^{-\nu-1}$ satisfies the same recurrence relation Eq. (3·3) as a_n^ν does. This shows that $R_{\rm C}^{-\nu-1}$ is also a homogeneous solution of the Teukolsky equation, which converges for $r > r_+$.

As for the homogeneous solution in a series of hypergeometric functions, which converges for $r < \infty$, the expansion coefficients satisfy the same three-term recurrence equation (3·3) derived by using a series of Coulomb wave functions. Thus one can use the same renormalized angular momentum ν to compute both series. This fact is important to match the solution in a series of Coulomb wave functions, which converges at infinity, with the one in a series of hypergeometric functions, which converges at the horizon. As a result of the matching, one can obtain the ingoing-wave solution $R_{lm\omega}^{\rm in}$, which converges in the entire region, as

$$R_{lm\omega}^{\rm in} = K_\nu R_{\rm C}^\nu + K_{-\nu-1} R_{\rm C}^{-\nu-1}, \tag{3·8}$$

where

$$\begin{aligned} K_\nu = {} & \frac{e^{i\epsilon}(2\epsilon)^{-2-\nu-N} 2^2 i^N \Gamma(3-2i\epsilon)\Gamma(N+2\nu+2)}{\Gamma(N+\nu+3+i\epsilon)\Gamma(N+\nu+1+i\epsilon)\Gamma(N+\nu-1+i\epsilon)} \\ & \times \left(\sum_{n=N}^{\infty} (-1)^n \frac{\Gamma(n+N+2\nu+1)}{(n-N)!} \frac{\Gamma(n+\nu-1+i\epsilon)\Gamma(n+\nu+1+i\epsilon)}{\Gamma(n+\nu+3-i\epsilon)\Gamma(n+\nu+1-i\epsilon)} a_n^\nu \right) \\ & \times \left(\sum_{n=-\infty}^{N} \frac{(-1)^n}{(N-n)!(N+2\nu+2)_n} \frac{(\nu-1-i\epsilon)_n}{(\nu+3+i\epsilon)_n} a_n^\nu \right)^{-1}, \end{aligned} \tag{3·9}$$

and N can be any integer. The factor K_ν is a constant to match the solutions in the overlap region of convergence and independent of the choice of N.

One can obtain analytic expressions for the asymptotic amplitudes $B_{lm\omega}^{\rm trans}$, $B_{lm\omega}^{\rm inc}$ and $B_{lm\omega}^{\rm ref}$ defined in Eq. (2·6) by comparing the asymptotic behavior of $R_{lm\omega}^{\rm in}$ Eq. (2·6) with Eq. (3·8) at $r^* \to \pm\infty$. They are derived as

$$B_{lm\omega}^{\rm trans} = \left(\frac{\epsilon}{\omega}\right)^{-4} \sum_{n=-\infty}^{\infty} a_n^\nu, \tag{3·10a}$$

$$B_{lm\omega}^{\rm inc} = \omega^{-1} \left[K_\nu - i e^{-i\pi\nu} \frac{\sin\pi(\nu+i\epsilon)}{\sin\pi(\nu-i\epsilon)} K_{-\nu-1} \right] A_+^\nu e^{-i\epsilon\ln\epsilon}, \tag{3·10b}$$

$$B_{lm\omega}^{\rm ref} = \omega^3 [K_\nu + i e^{i\pi\nu} K_{-\nu-1}] A_-^\nu e^{i\epsilon\ln\epsilon}, \tag{3·10c}$$

where

$$A_+^\nu = 2^{-3-i\epsilon} e^{-\frac{\pi\epsilon}{2}} e^{\frac{\pi}{2}i(\nu+3)} \frac{\Gamma(\nu+3+i\epsilon)}{\Gamma(\nu-1-i\epsilon)} \sum_{n=-\infty}^{+\infty} a_n^\nu, \tag{3·11a}$$

$$A_-^\nu = 2^{1+i\epsilon} e^{-\frac{\pi\epsilon}{2}} e^{-\frac{\pi}{2}i(\nu-1)} \sum_{n=-\infty}^{+\infty} (-1)^n \frac{(\nu-1-i\epsilon)_n}{(\nu+3+i\epsilon)_n} a_n^\nu. \tag{3·11b}$$

We summarize how to compute the gravitational waves using the MST formalism. One first should determine ν by solving Eq. (3·5). Then, one can compute the expansion coefficients a_n^ν using the continued fractions Eq. (3·6) for $n > 0$ and Eq. (3·7) for $n < 0$ with the condition $a_0^\nu = a_0^{-\nu-1} = 1$. Substituting the expansion coefficients a_n^ν into Eqs. (3·8) and (3·10), one can compute the ingoing-wave solution of the Teukolsky equation $R^{\rm in}_{\ell m\omega}$ and the asymptotic amplitudes $B^{\rm inc}_{\ell m\omega}$, which are necessary ingredients to compute $Z_{\ell m\omega}$ in Eq. (2·9) and hence allow one to compute the energy flux to infinity Eq. (2·11) and gravitational waveforms Eq. (2·12).

3.2. *Low frequency expansions of solutions*

In the practical calculation to determine ν, we solve an alternative equation which is equivalent to Eq. (3·5) for $n = 1$

$$\beta_0^\nu + \alpha_0^\nu R_1 + \gamma_0^\nu L_{-1} = 0, \tag{3·12}$$

where R_1 and L_{-1} are given by the continued fractions Eqs. (3·6) and (3·7) respectively.

In the following, we consider the low frequency approximation for Eq. (3·12). In the limit of low frequency, we solve Eq. (3·12) by requiring $\nu \to \ell$ for $\epsilon \to 0$. Since the orders of α_n^ν, γ_n^ν, β_n^ν, R_1 and L_{-1} in ϵ are $O(\epsilon)$, $O(\epsilon)$, $O(1)$, $O(\epsilon)$ and $O(\epsilon)$ respectively except for certain values of $n < 0$,[31),32)] one can systematically compute the low frequency expansion of ν. The closed analytic form of ν at $O(\epsilon^2)$ is given in Refs. 31) and 32). The expansion coefficients a_n^ν can be computed by using R_n and $L_{-|n|}$, whose order in ϵ are $O(\epsilon)$ for sufficiently large n. Therefore, the order of the expansion coefficients a_n^ν in ϵ are $O(\epsilon^{|n|})$ for sufficiently large $|n|$. Using the low frequency expansion of a_n^ν, one can easily derive that of the asymptotic amplitudes Eq. (3·10). Since the homogeneous solution of the Teukolsky equation $R^{\rm in}_{\ell m\omega}$ Eq. (3·8) is a function of $z = O(v)$ and $a_n^\nu \sim O(\epsilon^{|n|}) = O(v^{3\,|n|})$, the homogeneous solution is naturally related to the post-Newtonian approximation. For the calculation of $R^{\rm in}_{\ell m\omega}$ in the post-Newtonian approximation, however, one should add a larger number of terms in $R^\nu_{\rm C}$ Eq. (3·1) for $n < 0$ than that for $n > 0$. This is because the post-Newtonian order of a series of Coulomb wave functions for $n < 0$, $(a^\nu_{-|n|}F_{-|n|+\nu}(2\,i-\epsilon,z))/(a_0^\nu F_\nu(2\,i-\epsilon,z)) \sim O(v^{2\,|n|})$, grows slower than that for $n > 0$, $(a_n^\nu F_{n+\nu}(2\,i-\epsilon,z))/(a_0^\nu F_\nu(2\,i-\epsilon,z)) \sim O(v^{4\,n})$.[26)] Then, it is straightforward to compute the post-Newtonian expansion of the energy flux to infinity Eq. (2·11) and gravitational waveforms Eq. (2·12) using the post-Newtonian expansion of $Z_{\ell m\omega}$ Eq. (2·9). The closed analytic form of $Z_{\ell m\omega}$ at 2.5PN for the case of a test particle moving in circular orbits around a Schwarzschild black hole is given in Ref. 26).

§4. Comparison with numerical results

4.1. *Total energy flux to infinity*

Figure 1 shows the comparison of the energy flux to infinity between a high precision numerical calculation and post-Newtonian approximations up to 22PN. The numerical computation is based on a technique in Refs. 39) and 40). The accuracy of the numerical calculation is mainly limited by truncation of ℓ-mode. In this work we set $\ell = 25$ which gives relative error better than 10^{-14} up to the innermost stable circular orbit (ISCO). n-PN flux needs ℓ up to $n + 2$. We note that the agreement between the numerical energy flux and post-Newtonian energy flux becomes better when the PN order is higher even around ISCO. The relative error of the 22PN energy flux around ISCO is about 10^{-5} and an order of magnitude better than that of 14PN energy flux, which was derived in our previous paper.[27] We also note that the accuracy can be improved if we compute the energy flux using factorized resummation waveforms.[28] If one uses the factorized resummation waveforms, the relative error of the energy flux around ISCO can be reduced to 10^{-6} for 14PN expressions[27] and 10^{-7} for our 22PN expressions.

4.2. *Phase difference during two-year inspiral*

From Fig. 1, one may expect that 22PN expression for gravitational waves can be used for data analysis of EMRIs since the relative error with a high precision numerical calculation is about 10^{-5} around ISCO. To investigate the applicability of the PN expressions to the data analysis, we compute the phase difference during two years quasi-circular inspiral between the PN waveforms and the numerical waveforms. Following Ref. 41), we choose two systems, denoted as System-I (System-II), which correspond to the early (late) inspiral phase of an EMRI in the frequency band of eLISA. System-I has masses $(M, \mu) = (10^5, 10)M_\odot$ and inspirals from $r_0 \simeq 29M$ to $r_0 \simeq 16M$ with associated frequencies $f_{\rm GW} \in [4 \times 10^{-3}, 10^{-2}]$Hz. System-II has

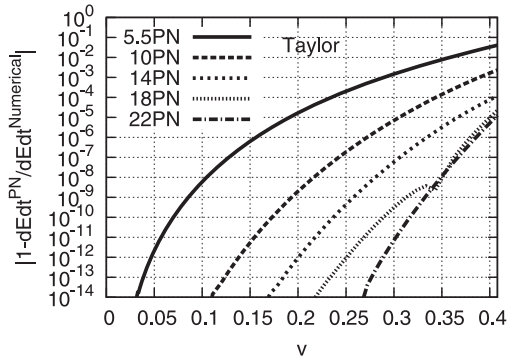

Fig. 1. Absolute values of the difference of the energy flux to infinity between numerical results and the PN approximation as a function of the orbital velocity. Note that the relative error of the energy flux between 22PN and the numerical calculation is an order of magnitude smaller than the one between 14PN and the numerical calculation even around ISCO, $v = 1/\sqrt{6} = 0.40825$.

masses $(M, \mu) = (10^6, 10)M_\odot$ and starts inspiral from $r_0 \simeq 11M$ to $r_0 \simeq 6.0M$ with frequencies $f_{\rm GW} \in [1.8 \times 10^{-3}, 4.4 \times 10^{-3}]$Hz. System-I (II) has the mass ratio of 10^{-4} (10^{-5}) and $\sim 1 \times 10^6$ ($\sim 5 \times 10^5$) rads of the orbital phase due to the two-year inspiral.

For the calculation of the phase, we use the method described in Ref. 42), which is also used in Refs. 26) and 41). The phase of the waveforms can be described as $m \int_0^t \Omega(t')dt' - \Psi_{\ell m}(t)$, where $\Omega(t) = \sqrt{M/r_0^3(t)}$ and $\Psi_{\ell m}$ is the phase of $Z_{\ell m\omega}$. To compute the radius of the orbits as a function of time $r_0(t)$, we use a interpolation method to save computational time. For the interpolation, using the total energy flux dE/dt induced by a particle we compute dr_0/dt for 10^3 points data of v from $v = 0.01$ to $v = 0.408$. Then, from the 10^3 points data of $(v,\ dr_0/dt)$, we compute $(r_0(t),\ \Psi_{\ell m}(t))$ using the cubic spline interpolation.[43)]

Figure 2 shows the absolute values of the phase difference of the dominant mode $h_{2,2}$ between the PN and the numerical calculation during the two-year inspiral. For System-I (II), the absolute values of the dephasing between the PN waveforms and the numerical waveforms after the two-year inspiral are about 4×10^1 (3×10^3), 9×10^{-3} (5×10^1), 10^{-5} (1), 8×10^{-9} (2×10^{-2}) and 10^{-9} (10^{-2}) rads for 5.5PN, 10PN, 14PN, 18PN and 22PN respectively. Using the factorized resummation waveforms, the absolute values of the phase difference for System-I (II) can be reduced to 3×10^{-8} (9×10^{-4}) rads for 14PN waveforms[27)] and 10^{-9} (10^{-4}) rads for our 22PN waveforms.

Since System-II represents the inspiral in the most strong-field of a Schwarzschild black hole, the dephase between the 22PN waveforms and the numerical waveforms after two-year inspirals is expected to be smaller than 10^{-2} rads for extreme mass ratio binaries in the frequency band of LISA. This may indicate that the 22PN waveforms will lead to the accuracy of the data analysis of EMRIs comparable to the one resulting from numerical waveforms.

4.3. *Hybrid formula of the energy flux to infinity for a Kerr black hole*

To investigate how higher post-Newtonian order terms for a non-spinning black hole improve the accuracy of the 4PN formula for a spinning black hole,[44)] we construct a hybrid formula for the energy flux in the post-Newtonian approximation by supplementing the 4PN energy flux for a Kerr black hole with our 22PN energy flux for a Schwarzschild black hole. In Figs. 3 and 4, n-PN energy flux includes n-PN energy flux to infinity for a Schwarzschild black hole and spin dependent terms of the 4PN expression for the energy flux to infinity for a Kerr black hole. The numerical flux for a Kerr black hole is computed using the same technique[39),40)] used in §4.1. For the numerical calculation, we set $\ell = 30$ which gives the relative error better than 10^{-5} up to ISCO for the parameters q used in Figs. 3 and 4.

In Fig. 3 (Fig. 4), the comparisons for $q > 0$ ($q < 0$) are shown. From these figures, one will find that for $|q| < 0.1$ adding higher post-Newtonian order terms for a non-spinning black hole achieves the accuracy that is about an order of magnitude better than the one using the 4PN expression of the energy flux for a spinning black hole. For $|q| \geq 0.1$, however, the improvement saturates when the PN order is higher than 8PN. For $q < -0.1$ the improvement becomes small when $|q|$ does large. For $q = -0.9$ one finds at most a factor of two improvement by adding the higher order

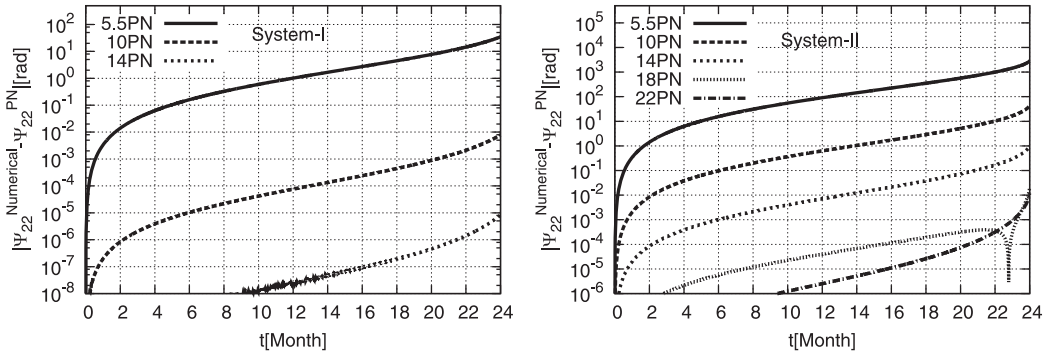

Fig. 2. Absolute values of the dephasing during the two-year inspiral between the PN and the numerical waveforms for the dominant $\ell = m = 2$ mode as a function of time in month. The left (right) panel represents the early (late) inspiral phase in the LISA band. The left panel shows the dephase for System-I of masses $(M, \mu) = (10^5, 10)M_\odot$, which evolves from $r_0 \simeq 29M$ to $r_0 \simeq 16M$ with associated frequencies $f_{\rm GW} \in [4 \times 10^{-3}, 10^{-2}]$Hz. The right panel shows the dephase for System-II of masses $(M, \mu) = (10^6, 10)M_\odot$, which explores the orbital radius in a region $r_0/M \in [6.0, 11]$ and frequencies in a range $f_{\rm GW} \in [1.8 \times 10^{-3}, 4.4 \times 10^{-3}]$Hz. Note that the dephase between the 18PN (22PN) waveforms and numerical waveforms for System-I due to the two-year inspiral is about 8×10^{-9} (10^{-9}) rads, which is below the lowest value of the dephase in the left panel. The dephase between the 22PN waveforms and numerical waveforms for System-II after the two-year inspiral is about 10^{-2} rads, which may suggest that the 22PN waveforms will provide the accuracy of the data analysis comparable to the one using numerical waveforms.

terms for a non-spinning black hole. For $q = 0.05$, the relative errors of the energy flux around ISCO are 2×10^{-1}, 4×10^{-2} and 6×10^{-3} for 4PN, 5.5PN and 8PN respectively. For $q = 0.05$, adding 8.5PN or higher order terms does not achieve better accuracy than adding 8PN terms, but achieves better accuracy than adding 5.5PN terms. For $q \geq 0.1$, adding higher post-Newtonian order terms for a non-spinning black hole does not always improve the accuracy. For $q = 0.1$, the relative errors of the 6PN energy flux around ISCO becomes larger than that of the 5.5PN energy flux around ISCO, but smaller than that of the 4PN energy flux around ISCO. For $q = 0.5$, the relative error of the 6PN energy flux around ISCO is almost the same as that of the 4PN energy flux around ISCO. For $q = 0.9$, the relative error of the 6PN (5.5PN) energy flux around ISCO is two times larger (an order of magnitude smaller) than that of the 4PN energy flux.

§5. Summary

Using a systematic method to compute homogeneous solutions of the Teukolsky equation,[32),33)] we have derived the 22PN expressions of gravitational waves for a test particle in circular orbits around a Schwarzschild black hole. The comparison of the energy flux between the PN expansion and high precision numerical results shows that the relative error of the 22PN energy flux around ISCO is about 10^{-5}. We also find that the dephase between the 22PN waveforms and the numerical

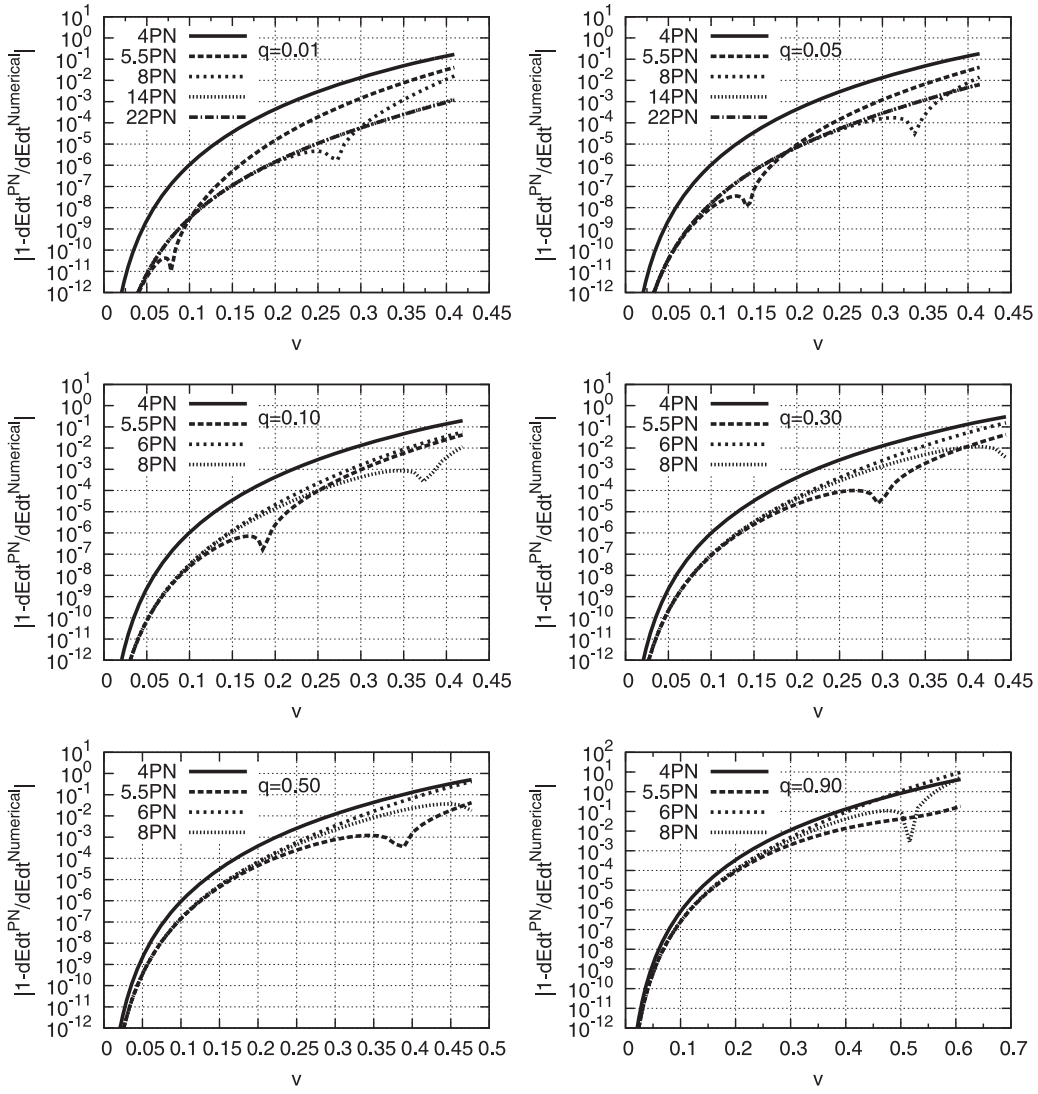

Fig. 3. Absolute values of the difference of the energy flux to infinity between numerical results and the PN approximation as a function of the orbital velocity, $v = (M/r_0)^{1/2}[1 + q\,(M/r_0)^{3/2}]^{-1/3}$, up to ISCO for $q = 0.01$, 0.05, 0.1, 0.3, 0.5 and 0.9. The energy flux at n-PN combines the n-PN energy flux for a Schwarzschild black hole and spin dependent terms of the 4PN energy flux for a Kerr black hole.[44] For $q < 0.1$, higher PN order terms for a non-spinning black hole improve the relative accuracy of the energy flux. For $q \geq 0.1$, however, higher PN order terms for a non-spinning black hole do not always improve the accuracy although one can find the accuracy of some PN order is an order of magnitude better than that of the 4PN energy flux.

waveforms after the two-year inspiral will be smaller than 10^{-2} rads for the most of the parameter space of EMRIs. This may imply that the 22PN waveforms will provide the accuracy in the LISA-type data analysis comparable to the one using high precision numerical waveforms. (See Ref. 27) for the same discussion using factorized resummed waveforms, developed in Ref. 28), at 14PN.)

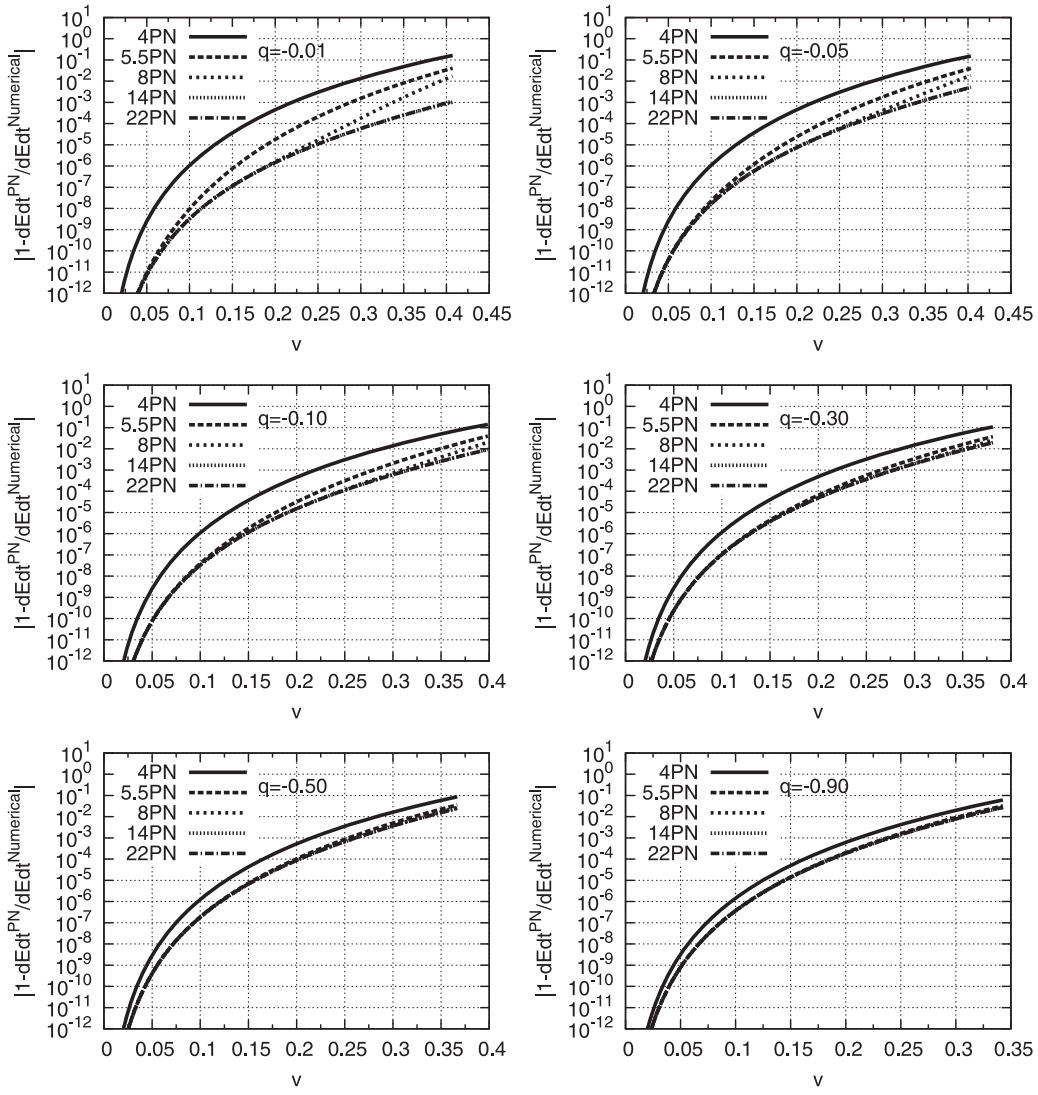

Fig. 4. Same as Fig. 3 but for $q = -0.01, -0.05, -0.1, -0.3, -0.5$ and $q = -0.9$. For $|q| < 0.1$, adding higher post-Newtonian order terms for a non-spinning black hole achieves the accuracy that is about an order of magnitude better than the one using the 4PN energy flux for a spinning black hole. For $q < -0.1$ the improvement becomes small when $|q|$ does large.

The next application will be the case in which a particle moves in circular orbits around a Kerr black hole. The current available result for the case is 4PN,[44] which gives the relative errors of 10^{-1} ($O(1)$) for $q = 0.1$ ($q = 0.9$) around ISCO (see Figs. 3 and 4). To investigate whether our 22PN formula of the energy flux improves the accuracy for the case of a Kerr black hole, we construct a hybrid formula of the energy flux by supplementing the 4PN energy flux for a Kerr black hole with the 22PN energy flux for a Schwarzschild black hole. We found that for $q < 0.1$ non-spinning terms of higher post-Newtonian order expressions improve the

accuracy around ISCO. However, since for $q \geq 0.1$ non-spinning terms of higher post-Newtonian order expressions of the total energy flux do not always improve the accuracy for a large value of the spin, it is necessary to obtain high PN order expressions for the case of a Kerr black hole. For $q = 0.9$, the numerical calculation shows that one needs to include $\ell = 30$ modes to achieve the relative error of the total energy flux as 10^{-5} around ISCO (see §4.3). This may indicate that we need to compute at least up to 28PN to obtain the relative error of 10^{-5} around ISCO for $q = 0.9$. It may be difficult to perform such a high post-Newtonian order calculation using our current code since the number of terms necessary to derive the PN expressions grows exponentially when the PN order becomes higher (see §1 and Ref. 27)). If one cannot obtain sufficiently high post-Newtonian order expressions, another approach may be the effective-one-body formalism which can include unknown coefficients in the post-Newtonian expressions by calibrating them with numerical results.[41),45)]

Acknowledgements

It is a pleasure to thank Bala R. Iyer for continuous encouragement to look into this problem and useful comments on the manuscript. The author is grateful for the support of the European Union FEDER funds, the Spanish Ministry of Economy and Competitiveness (projects FPA2010-16495 and CSD2007-00042) and the Conselleria d'Economia Hisenda i Innovacio of the Govern de les Illes Balears.

Appendix A

—— 7PN Formula for the Energy Flux to Infinity ——

The total energy flux to infinity at 7PN becomes

$$\begin{aligned}
\frac{dE}{dt} =& \left(\frac{dE}{dt}\right)_N \left[1 - \frac{1247}{336}v^2 + 4\,\pi v^3 - \frac{44711}{9072}v^4 - \frac{8191}{672}\,\pi v^5\right.\\
&+ \left\{\frac{6643739519}{69854400} - \frac{1712}{105}\,\gamma - \frac{3424}{105}\,\ln(2) + \frac{16}{3}\,\pi^2 - \frac{1712}{105}\,\ln(v)\right\} v^6 - \frac{16285}{504}\,\pi v^7\\
&+ \left\{-\frac{323105549467}{3178375200} + \frac{232597}{4410}\,\gamma + \frac{39931}{294}\,\ln(2) - \frac{1369}{126}\,\pi^2 - \frac{47385}{1568}\,\ln(3)\right.\\
&\quad \left.+\frac{232597}{4410}\,\ln(v)\right\} v^8\\
&+ \left\{\frac{265978667519}{745113600}\,\pi - \frac{13696}{105}\,\ln(2)\,\pi - \frac{6848}{105}\,\pi\,\gamma - \frac{6848}{105}\,\pi\,\ln(v)\right\} v^9\\
&+ \left\{-\frac{2500861660823683}{2831932303200} + \frac{916628467}{7858620}\,\gamma - \frac{83217611}{1122660}\,\ln(2) - \frac{424223}{6804}\,\pi^2\right.\\
&\quad \left.+\frac{47385}{196}\,\ln(3) + \frac{916628467}{7858620}\,\ln(v)\right\} v^{10}\\
&+ \left\{\frac{177293}{1176}\,\pi\,\gamma + \frac{8521283}{17640}\,\ln(2)\,\pi + \frac{8399309750401}{101708006400}\,\pi - \frac{142155}{784}\,\pi\,\ln(3)\right.
\end{aligned}$$

$$
\begin{aligned}
&+\frac{177293}{1176}\,\pi\ln(v)\Bigg\}v^{11}\\
&+\Bigg\{-\frac{256}{45}\,\pi^4-\frac{37744140625}{260941824}\,\ln(5)+\frac{2067586193789233570693}{602387400044430000}\\
&-\frac{246137536815857}{157329572400}\,\gamma-\frac{27392}{105}\,\zeta(3)-\frac{437114506833}{789268480}\,\ln(3)\\
&-\frac{271272899815409}{157329572400}\,\ln(2)+\frac{5861888}{11025}\,\ln(2)\,\gamma-\frac{54784}{315}\,\ln(2)\,\pi^2\\
&+\frac{3803225263}{10478160}\,\pi^2-\frac{27392}{315}\,\pi^2\,\gamma+\frac{5861888}{11025}\,\ln(2)^2+\frac{1465472}{11025}\,\gamma^2\\
&+\left(\frac{2930944}{11025}\,\gamma-\frac{27392}{315}\,\pi^2-\frac{246137536815857}{157329572400}+\frac{5861888}{11025}\,\ln(2)\right)\ln(v)\\
&+\frac{1465472}{11025}\,\ln(v)^2\Bigg\}v^{12}\\
&+\Bigg\{\frac{300277177}{436590}\,\pi\,\gamma-\frac{81605095538444363}{20138185267200}\,\pi-\frac{42817273}{71442}\,\ln(2)\,\pi\\
&+\frac{142155}{98}\,\pi\,\ln(3)+\frac{300277177}{436590}\,\pi\ln(v)\Bigg\}v^{13}\\
&+\Bigg\{\frac{531077}{2205}\,\zeta(3)+\frac{19402232550751339}{17896238860500}\,\ln(2)\\
&+\frac{58327313257446476199371189}{8332222517414555760000}+\frac{128223}{245}\,\ln(2)\,\pi^2-\frac{9523}{945}\,\pi^4\\
&-\frac{5811697}{2450}\,\ln(2)^2+\frac{1848015}{2744}\,\gamma\ln(3)-\frac{471188717}{231525}\,\ln(2)\,\gamma\\
&-\frac{6136997968378863}{1256910054400}\,\ln(3)+\frac{9926708984375}{5088365568}\,\ln(5)\\
&+\frac{1848015}{2744}\,\ln(2)\,\ln(3)-\frac{142155}{392}\ln(3)\,\pi^2+\frac{9640384387033067}{17896238860500}\,\gamma\\
&-\frac{52525903}{154350}\,\gamma^2+\frac{531077}{6615}\,\pi^2\,\gamma+\frac{2621359845833}{2383781400}\,\pi^2+\frac{1848015}{5488}\,\ln(3)^2\\
&+\left(\frac{9640384387033067}{17896238860500}-\frac{471188717}{231525}\,\ln(2)+\frac{531077}{6615}\,\pi^2-\frac{52525903}{77175}\,\gamma\right.\\
&\left.+\frac{1848015}{2744}\,\ln(3)\right)\ln(v)-\frac{52525903}{154350}\,\ln(v)^2\Bigg\}v^{14}\Bigg],
\end{aligned}
$$

where γ is the Euler constant and $\zeta(n)$ is the Zeta function.

We note that coefficients in the post-Newtonian expansion for the total energy flux are polynomial functions of π, γ, $\ln(n)$, $\ln(v)$ and $\zeta(n)$. One will find that the coefficient at 1.5PN, 4π, is derived from the PN expansion of $e^{-\pi\epsilon/2}$ in Eq. (3·11a) for $\ell = m = 2$ mode. One will also find that γ, $\ln(2)$ and $\ln(v)$ terms at 3PN and $\zeta(3)$ term at 6PN are derived by the PN expansion of the homogeneous Teukolsky

solution in a series of Coulomb wave functions Eq. (3·1) for $\ell = m = 2$ mode. Similarly, one will find that $\ln(n)$ and $\zeta(2n-1)$ terms appear from $(n+1)$-PN and $3n$-PN respectively (see Ref. 29)). We also note that $(\ln(v))^n$ terms appear from $3n$-PN (see Appendix B and Ref. 29)). One of the reasons is that $(\ln(v))^n$ terms at $3n$-PN are produced by the PN expansion of z^ν in the homogeneous Teukolsky solution in a series of Coulomb wave functions Eq. (3·1), where $z = \omega r = O(v)$ and $\nu = \ell + \nu^{(2)}\, v^6 + O(v^9)$. Noting that the energy flux is computed by the square of the homogeneous Teukolsky solution and $\nu^{(2)} = -856/105$ for the dominant mode $\ell = m = 2$,[31)–33)] one can estimate leading $(\ln(v))^n$ terms in the energy flux using series expansion of $v^{-1712/105}\, v^6$ and find that these $(\ln(v))^n$ terms at $3n$-PN agree with the ones in our 22PN energy flux. The explicit expressions for these leading $(\ln(v))^n$ terms at $3n$-PN are already derived in Eq. (44) of Ref. 46) using the renormalization group equations and agree with the ones in our 22PN energy flux.

Appendix B

22PN Energy Flux to Infinity for Numerical Calculation

The total energy flux to infinity at 22PN, which can be used for numerical calculation for double precision calculation, becomes

$$\begin{aligned}
\frac{dE}{dt} = \left(\frac{dE}{dt}\right)_N \Bigg[& 1 - 3.7113095238095238\, v^2 + 12.566370614359173\, v^3 \\
& - 4.9284611992945326\, v^4 - 38.292835454693446\, v^5 \\
& + \{115.73171667561132 - 16.304761904761905\, \ln(v)\}\, v^6 \\
& - 101.50959595974163\, v^7 \\
& + \{-117.50439072267733 + 52.743083900226757\, \ln(v)\}\, v^8 \\
& + \{719.12834223342969 - 204.89168087412289\, \ln(v)\}\, v^9 \\
& + \{-1216.9069913170420 + 116.63987659410940\, \ln(v)\}\, v^{10} \\
& + \{958.93497011956684 + 473.62447817423062\, \ln(v)\}\, v^{11} \\
& + \{2034.7899821303756 - 1900.7293251880964\, \ln(v) \\
& + 132.92263038548753\, \ln(v)^2\}\, v^{12} \\
& + \{-7781.9735576745461 + 2160.7196071918322\, \ln(v)\}\, v^{13} \\
& + \{15384.154335011960 + 267.42096713731240\, \ln(v) \\
& - 340.30387431162941\, \ln(v)^2\}\, v^{14}
\end{aligned}$$

$$
\begin{aligned}
&+\{-12154.148413021627-10431.406072327709\ln(v)\\
&+1670.3550364595162\ln(v)^2\}v^{15}\\
&+\{-14423.548835921780+21798.970641540720\ln(v)\\
&-1259.2120782299356\ln(v)^2\}v^{16}\\
&+\{89501.573309687739-29246.578925458487\ln(v)\\
&-2162.0533013852443\ln(v)^2\}v^{17}\\
&+\{-183583.88710261773-6836.8321880197775\ln(v)\\
&+14856.770074354592\ln(v)^2-722.42394673001476\ln(v)^3\}v^{18}\\
&+\{232409.13476410614+94495.266713306094\ln(v)\\
&-20805.243844022191\ln(v)^2\}v^{19}\\
&+\{29936.08409119159-292760.39953957798\ln(v)\\
&+16701.438906657108\ln(v)^2+1179.1301184451609\ln(v)^3\}v^{20}\\
&+\{-825753.06115027078+441939.66010505905\ln(v)\\
&+57856.092251923344\ln(v)^2-9078.2470552974338\ln(v)^3\}v^{21}\\
&+\{2458416.5416899955-398672.73444594275\ln(v)\\
&-158992.86702314628\ln(v)^2+8194.4543122810763\ln(v)^3\}v^{22}\\
&+\{-3952774.9138307063-759261.92414463453\ln(v)\\
&+360084.58553892898\ln(v)^2-897.89185596522682\ln(v)^3\}v^{23}\\
&+\{2976918.2174426533+3500957.1806440358\ln(v)\\
&-318467.34660011464\ln(v)^2-70899.505625286470\ln(v)^3\\
&+2944.7376114328221\ln(v)^4\}v^{24}\\
&+\{7019236.3677905130-8886564.3632113352\ln(v)
\end{aligned}
$$

$$+52809.58085577387\,\ln(v)^2+113193.57722837660\,\ln(v)^3\big\}\,v^{25}$$

$$+\{-31202976.107218423+11762892.421868797\,\ln(v)$$

$$+1982484.3746860539\,\ln(v)^2-220750.96927550645\,\ln(v)^3$$

$$-1067.0133724433031\,\ln(v)^4\big\}\,v^{26}$$

$$+\{68807279.901880549-2488093.498633921\,\ln(v)$$

$$-5652341.0354988102\,\ln(v)^2-45136.07364771081\,\ln(v)^3$$

$$+37004.664187307634\,\ln(v)^4\big\}\,v^{27}$$

$$+\{-79540420.970120669-47212469.571473335\,\ln(v)$$

$$+13096024.087086880\,\ln(v)^2+336827.97427818428\,\ln(v)^3$$

$$-34129.747458105155\,\ln(v)^4\big\}\,v^{28}$$

$$+\{-25925436.707911899+148981108.02576149\,\ln(v)$$

$$-12498185.772224907\,\ln(v)^2-2301205.5277433290\,\ln(v)^3$$

$$+74157.041397297642\,\ln(v)^4\big\}\,v^{29}$$

$$+\{402444362.19171711-278017845.54926934\,\ln(v)$$

$$-11687734.115250883\,\ln(v)^2+4307818.2864565577\,\ln(v)^3$$

$$+213688.37579621078\,\ln(v)^4-9602.6491252818883\,\ln(v)^5\big\}\,v^{30}$$

$$+\{-1071349694.3775396+204222856.19303166\,\ln(v)$$

$$+116030090.57483748\,\ln(v)^2-10073180.152647150\,\ln(v)^3$$

$$-291438.02818774543\,\ln(v)^4\big\}\,v^{31}$$

$$+\{1626083110.9818554+488335019.02563548\,\ln(v)$$

$$-291331989.87961219\,\ln(v)^2+2942116.4939216327\,\ln(v)^3$$

$$+1469109.8755678809\,\ln(v)^4-13190.813005345736\,\ln(v)^5\big\}\,v^{32}$$

$$+\{-544918059.05664234-2428299657.0865688\,\ln(v)$$

$$
\begin{aligned}
&+456879101.34472726\,\ln(v)^2 + 26594005.608730906\,\ln(v)^3 \\
&-1380784.1214801066\,\ln(v)^4 - 120670.44778794414\,\ln(v)^5\big\}\,v^{33} \\
&+\big\{-4616517093.2988715 + 5243279919.6114690\,\ln(v) \\
&-38163582.107515614\,\ln(v)^2 - 148107440.84908515\,\ln(v)^3 \\
&+4207389.1083361737\,\ln(v)^4 + 75160.959023984080\,\ln(v)^5\big\}\,v^{34} \\
&+\big\{15817926503.756157 - 6113621574.3296087\,\ln(v) \\
&-1759324394.0096811\,\ln(v)^2 + 301378311.00479927\,\ln(v)^3 \\
&+5936380.6862923426\,\ln(v)^4 - 556060.02405979572\,\ln(v)^5\big\}\,v^{35} \\
&+\big\{-28150296022.364384 - 3508984690.6951288\,\ln(v) \\
&+6000317955.561223\,\ln(v)^2 - 384692002.27108097\,\ln(v)^3 \\
&-22068300.433686751\,\ln(v)^4 - 341412.56352301983\,\ln(v)^5 \\
&+26094.817940448560\,\ln(v)^6\big\}\,v^{36} \\
&+\big\{21923504375.507727 + 35127491396.323879\,\ln(v) \\
&-10561491802.698468\,\ln(v)^2 - 475718215.99686552\,\ln(v)^3 \\
&+111153302.13498037\,\ln(v)^4 - 796270.98236252163\,\ln(v)^5\big\}\,v^{37} \\
&+\big\{45025396338.391247 - 92707192688.847145\,\ln(v) \\
&+7698249771.7266011\,\ln(v)^2 + 2977537585.1450740\,\ln(v)^3 \\
&-169371453.19161573\,\ln(v)^4 - 6119765.2693920173\,\ln(v)^5 \\
&+97766.114767012667\,\ln(v)^6\big\}\,v^{38} \\
&+\big\{-214410246975.35927 + 133503754160.33392\,\ln(v) \\
&+23775901926.064545\,\ln(v)^2 - 8155501690.3403790\,\ln(v)^3 \\
&+154065244.97484914\,\ln(v)^4 + 9046986.8078241302\,\ln(v)^5
\end{aligned}
$$

$$
\begin{aligned}
&+327917.15335390533\,\ln(v)^6\big\}\,v^{39}\\
&+\{457980639365.70258-27000183902.801376\,\ln(v)\\
&-105502717126.40338\,\ln(v)^2+10988802554.611972\,\ln(v)^3\\
&+812919382.11642567\,\ln(v)^4-51924388.655256156\,\ln(v)^5\\
&+120256.87755099946\,\ln(v)^6\big\}\,v^{40}\\
&+\{-514130514219.36581-465015514007.42288\,\ln(v)\\
&+229651541194.18049\,\ln(v)^2+80213128.550237347\,\ln(v)^3\\
&-2851170970.3905610\,\ln(v)^4+29259922.934207013\,\ln(v)^5\\
&+2678253.6091283655\,\ln(v)^6\big\}\,v^{41}\\
&+\{-246285643927.15478+1492672221227.6888\,\ln(v)\\
&-247860628603.14260\,\ln(v)^2-55696072359.371755\,\ln(v)^3\\
&+6850753270.3130100\,\ln(v)^4-23989989.755180755\,\ln(v)^5\\
&+52812.42772484907\,\ln(v)^6-60781.399066731884\,\ln(v)^7\big\}\,v^{42}\\
&+\{2724640759315.9973-2613409597570.6299\,\ln(v)\\
&-213879053529.96990\,\ln(v)^2+171699406240.25908\,\ln(v)^3\\
&-5303254029.5716242\,\ln(v)^4-666793776.26385442\,\ln(v)^5\\
&+13432837.504069723\,\ln(v)^6\big\}\,v^{43}\\
&+\{-7046976172838.4569+1802703723560.9900\,\ln(v)\\
&+1747504187818.0615\,\ln(v)^2-311569476082.28712\,\ln(v)^3\\
&-11182012302.436379\,\ln(v)^4+1624600040.7560485\,\ln(v)^5\\
&+15277409.847611050\,\ln(v)^6-424858.25453008154\,\ln(v)^7\big\}\,v^{44}\Big].
\end{aligned}
$$

References

1) G. M. Harry for the LIGO Scientific Collaboration, Class. Quantum Grav. **27** (2010), 084006.
2) F. Acernese et al., Class. Quantum Grav. **25** (2008), 184001.
3) K. Somiya, Class. Quantum Grav. **29** (2012), 124007.
4) L. Blanchet, Living Rev. Relativity **9** (2006), 4, http://relativity.livingreviews.org/Articles/lrr-2006-4
5) T. Damour, P. Jaranowski and G. Schäfer, Phys. Lett. B **513** (2001), 147.
6) L. Blanchet, T. Damour and G. Esposito-Farese, Phys. Rev. D **69** (2004), 124007.
7) L. Blanchet, G. Faye, B. R. Iyer and B. Joguet, Phys. Rev. D **65** (2002), 061501(R).
8) L. Blanchet, T. Damour, G. Esposito-Farèse and B. R. Iyer, Phys. Rev. Lett. **93** (2004), 091101.
9) L. E. Kidder, Phys. Rev. D **77** (2008), 044016.
10) L. Blanchet, G. Faye, B. R. Iyer and S. Sinha, Class. Quantum Grav. **25** (2008), 165003.
11) M. Favata, Phys. Rev. D **80** (2009), 024002.
12) G. Faye, S. Marsat, L. Blanchet and B. R. Iyer, arXiv:1204.1043.
13) M. Hannam, Class. Quantum Grav. **26** (2009), 114001.
14) I. Hinder, Class. Quantum Grav. **27** (2010), 114004.
15) A. Buonanno et al., Phys. Rev. D **76** (2007), 104049.
16) P. Ajith et al., Phys. Rev. D **77** (2008), 104017.
17) P. Amaro-Seoane et al., arXiv:1201.3621.
18) E. Poisson, Phys. Rev. D **47** (1993), 1497.
19) E. Poisson, A. Pound and I. Vega, Living Rev. Relativity **14** (2011), 7, http://www.livingreviews.org/lrr-2011-7
20) L. Barack, Class. Quantum Grav. **26** (2009), 213001.
21) J. Thornburg, arXiv:1102.2857.
22) C. Cutler, L. S. Finn, E. Poisson and G. J. Sussman, Phys. Rev. D **47** (1993), 1511.
23) H. Tagoshi and T. Nakamura, Phys. Rev. D **49** (1994), 4016.
24) H. Tagoshi and M. Sasaki, Prog. Theor. Phys. **92** (1994), 745.
25) T. Tanaka, H. Tagoshi and M. Sasaki, Prog. Theor. Phys. **96** (1996), 1087.
26) R. Fujita and B. R. Iyer, Phys. Rev. D **82** (2010), 044051.
27) R. Fujita, Prog. Theor. Phys. **127** (2012), 583.
28) T. Damour, B. R. Iyer and A. Nagar, Phys. Rev. D **79** (2009), 064004.
29) http://www2.yukawa.kyoto-u.ac.jp/~misao/BHPC/index.html
30) S. A. Teukolsky, Astrophys. J. **185** (1973), 635.
31) M. Sasaki and H. Tagoshi, Living Rev. Relativity **6** (2003), 6, http://relativity.livingreviews.org/Articles/lrr-2003-6
32) S. Mano, H. Suzuki and E. Takasugi, Prog. Theor. Phys. **95** (1996), 1079.
33) S. Mano and E. Takasugi, Prog. Theor. Phys. **97** (1997), 213.
34) H. Tagoshi, S. Mano and E. Takasugi, Prog. Theor. Phys. **98** (1997), 829.
35) N. Sago, T. Tanaka, W. Hikida, K. Ganz and H. Nakano, Prog. Theor. Phys. **115** (2006), 873.
36) K. Ganz, W. Hikida, H. Nakano, N. Sago and T. Tanaka, Prog. Theor. Phys. **117** (2007), 1041.
37) Y. Pan, A. Buonanno, R. Fujita, E. Racine and H. Tagoshi, Phys. Rev. D **83** (2011), 064003.
38) Ed. M. Abramowitz and I. A. Stegun, *Handbook of Mathematical Functions* (Dover, New York, 1972), Chap. 13.
39) R. Fujita and H. Tagoshi, Prog. Theor. Phys. **112** (2004), 415.
40) R. Fujita and H. Tagoshi, Prog. Theor. Phys. **113** (2005), 1165.
41) N. Yunes, A. Buonanno, S. A. Hughes, M. C. Miller and Y. Pan, Phys. Rev. Lett. **104** (2010), 091102.
42) S. A. Hughes, Phys. Rev. D **64** (2001), 064004.
43) W. H. Press, S. A. Teukolsky, W. T. Vetterling and B. P. Flannery, *Numerical Recipes in C* (Cambridge University Press, Cambridge, England, 1992).

44) H. Tagoshi, M. Shibata, T. Tanaka and M. Sasaki, Phys. Rev. D **54** (1996), 1439.
45) N. Yunes, A. Buonanno, S. A. Hughes, Y. Pan, E. Barausse, M. C. Miller and W. Throwe, Phys. Rev. D **83** (2011), 044044.
46) W. D. Goldberger and A. Ross, Phys. Rev. D **81** (2010), 124015.